Microchimica Acta
https://doi.org/10.1007/s00604-019-3280-5

ORIGINAL PAPER

Electrochemiluminescent determination of the activity of uracil-DNA glycosylase: Combining nicking enzyme assisted signal amplification and catalyzed hairpin assembly

Qiao Liu[1] · Chao Liu[1] · Guang Zhu[1] · Haifeng Xu[1] · Xiao Jie Zhang[1] · Chongju Hu[1] · Yong Xie[1] · Keying Zhang[1] · Hongyan Wang[1]

Received: 29 October 2018 / Accepted: 23 January 2019

Abstract

An electrochemiluminescence (ECL) based method is described for the determination of the activity of the enzyme uracil-DNA glycosylase (UDG). It is based on the use of nicking enzyme-assisted signal amplification and catalytic hairpin assembly. UDG can recognize and hydrolyze the uracil bases from the stem of hairpin DNA1 (HP1). This causes the opening of HP1 to form a straight strand DNA. The straight HP1 can hybridize with hairpin DNA2 (HP2) to form a DNA duplex. In the presence of nicking enzyme, it can recognize and cut the specific sequences in the HP2 of the DNA duplex, and a subsequent release of HP1. It hybridizes with other HP2 to trigger the continuous cleavage of HP2, concomitantly generating abundant intermediate sequences (S1). The hairpin DNA3 (HP3) is immobilized on a gold electrode via Au-S chemistry. In the presence of S1, HP3 hybridizes with S1 and its hairpin structure is opened. This hybridization causes displacement from hairpin DNA4 (HP4), and S1 is released to initiate the next hybridization process. Thus, a massive number of HP3-HP4 duplexes is generated after the cyclic process. Subsequently, the cDNA modified on bio-bar-coded AuNP-CdSe quantum dots are immobilized on the electrode by hybridization with the redundant part of the opened HP4. This results in a significant amplification of the ECL signal. This biosensor is sensitive and selective for UDG. The detection limit is 6 $mU \cdot mL^{-1}$ and the dynamic range extends from 0.02 to 22 $U \cdot mL^{-1}$. The method was applied to real samples and gained good performance, thereby providing an ideal way for DNA repair enzyme-related biomedical research and diagnosis.

Keywords Electrochemiluminescence · Biosensor · Catalyzed hairpin assembly · Uracil-DNA glycosylase · Signal amplification

Introduction

The genome is made up of specific pairs of DNA bases, and their stabilization and veracity are precondition for all living things. Nevertheless, the structure of DNA base can be destroyed by various environmental factors, such as ultraviolet radiation, genetic toxic chemicals and ionizing radiation, resulting in the instability of the genome and induction of carcinogenesis [1–3]. Uracils are a universally found destroyed base in DNA, which arise from dUMP substituting dTMP and the desamination of cytosine residues in DNA synthesis process [4, 5]. On the other hand, the cytosine desamination is more likely to cause the formation of U:G base pair in the double helix DNA, ultimately resulting in the mutation of G:C base pair to A:T base pair [6]. The uracil bases in single-stranded and double-stranded DNA are usually restored by highly specific uracil DNA glycosylase (UDG) by means of base excision repair (BER) process [7]. UDG can specifically recognize the uracil lesions in DNA by cleaving the N-glycosidic bond between the uracil and DNA backbone, resulting in generation of an abasic site (AP site) and cooperating with else repair enzymes to achieve entire DNA repair [8–10]. Inactivity of UDG will interrupt the BER process and result in various diseases including

Qiao Liu and Chao Liu contributed equally to this work.

Electronic supplementary material The online version of this article (https://doi.org/10.1007/s00604-019-3280-5) contains supplementary material, which is available to authorized users.

✉ Keying Zhang
zhangky1983@163.com

✉ Hongyan Wang
suzhouwhy@163.com

[1] Anhui Key Laboratory of Spin Electron and Nanomaterials, School of Chemistry and Chemical Engineering, Suzhou University, Suzhou 234000, People's Republic of China

Published online: 15 February 2019

neurodegeneration, prostate tumor, lymphoma, human immunodeficiencys [11, 12]. Therefore, the accurate and sensitive assay of UDG activity is conducive to the study of fundamental diagnosis and clinical biomedical research.

At present, various kinds of means have been put forward to analyze UDG activity including gel electrophoresis [13, 14], radioactive labeling and fluorescent methods [15, 16]. Although those methods were widely used, they still possessed some weakness including low sensitivity and bad reproducibility. Therefore, developing a simple, convenient and sensitive detection means for UDG is extremely required. So far, electrochemiluminescence (ECL) with the merits of high sensitivity, simple equipment, low background noise and spatial mobility, is a luminous emission that stimulated via excited electrons jumping to ground state [17, 18]. Although the ECL technique has attracted particular attention and been widely used in the fields of RNA analysis [19, 20], immunoassays [21, 22], toxins detection [23, 24], the UDG based on ECL assay are scarcely been reported.

Nicking endonucleases (NEases) are a special group of restriction endonucleases, which are able to identify specific nucleotide sequences in double stranded DNA and just cut single strand of a double stranded DNA at a specific position known as a restriction site [25, 26]. Recently, in order to fully exploit these attractive traits of NEases, many researches have been developed different NEases assisted signal amplification detection platforms for various analytes to improve the sensitivity [27, 28]. Meanwhile, to further heighten the sensitivity of UDG activity detection, NEases catalyzed signal amplification techniques have been used for more sensitive UDG activity assay. For instance, Liu's group proposed a strategy for UDG detection by utilizing colorimetric assay method based on enzyme-assisted signal amplification [29]. Wang's group designed a simple fluorescent strategy to detection of UDG activity and achieved ultrasensitive detection by coupling with excision repair-initiated enzyme-assisted multiple signal amplification [16]. In addition, strand-displacement amplification (SDA) and rolling circle amplification (RCA) have been used successfully for ultrasensitive detection of UDG because of the outstanding merits of admirable specificity and high sensitivity [30–32]. However, the performance is not completely satisfied owing to their linear amplification characteristic. Currently, target-catalyzed hairpin assembly (CHA) is widely applied all kinds of biomolecule assays such as DNA, microRNA and proteins because it possesses high amplification efficiency and speedy amplification kinetics [33–35]. CHA is a fine non-enzymatic amplification technique, where a pair of hairpins DNA are catalyzed to form double-stranded DNA when an initiator strand is inputted, by using CHA reaction, catalytic amplification can be achieved hundred-fold [36]. As far as we know, there are few reports about the ECL detection methods which combine the two amplification strategies of nicking enzyme assisted signal and catalyzed hairpin assembly. Inspired by the above-mentioned fact, we challenged to integrate with two amplification strategies to develop a new ECL biosensor system.

The biobar-coded nanoprobe as an amplified platform plays a significant role in achieving the development of highly sensitive biosensors. Especially, Au NPs, have drew a lot of attention due to their unique properties, such as larger specific surface area, biocompatibility and stability [37]. A great deal of thiolated DNA can be closely bound on the surface of Au NPs by Au-thiol bond. However, signal probes modified different functional groups can connect with the other side of DNA stand to achieve amplified signals. Hence, to further improve the sensitivity, the amplification by biobar-coded Au NPs connecting with QDs is an ideal way to fabricate ECL biosensors.

Herein, taking advantages of the combination of nicking enzyme assisted signal amplification and catalyzed hairpin assembly, we designed multiple amplified ECL sensing strategy to detect UDG based on bio-bar-coded Au NP-CdSe QDs serve as the ECL signal probes. Firstly, the removal of uracil by UDG triggered the nicking enzyme assisted signal amplification in first-step amplification, which played the important role for generation of abundant intermediate sequences (S1). Subsequently, under the participation of hairpin DNA 4 (HP4), the S1 interacts with hairpin DNA3 (HP3) on the electrode. This catalyzes the hairpin assembly induced signal amplification. Ultimately, the cDNA modified bio-bar-coded Au NP-CdSe QDs further connected with residual single stranded fragment of HP4 to get the final amplified ECL signal. With the above signal amplification strategies, the biosensor presented an extremely wide detection range and approving sensitivity for UDG detection, and providing a hopeful way for the determination of UDG in clinical diagnosis.

Experimental

Materials and reagents

$CdCl_2 \cdot 2.5H_2O$ (98%) and trisodium citrate ($Na_3C_6H_5O_7 \cdot 2H_2O$) were purchased from Sinopharm Chemical Reagent Co., Ltd. (China). selenium powder (99.9%) and L-Cysteine (L-Cys) were bought from Shanghai Reagent Company (Shanghai, China). Tri-(2-carboxyethyl) phosphine hydrochloride (TCEP), Chloroauric acid ($HAuCl_4$), N-(3-Dimethylaminopropyl)-N′-ethylcarbodiimide hydrochloride (EDC) and N-Hydroxysuccinimide (NHS) were purchased from sigma-aldrich (Shanghai, China). Endonuclease (Nb.BbvCI, 10,000 $U \cdot mL^{-1}$) and Uracil-DNA glycosylase (UDG) were provided from New England Biolabs (USA). 6-mercapto-1-hexanol (MCH) was supplied from J&K Scientific Ltd. (Beijing, China). All oligonucleotides with purification were synthesized

by Sangon Biotech Co., Ltd. (Shanghai, China) in this work. These sequences are shown in Table 1.

10 mM Tris-HCl (pH 7.4, 1.0 mM EDTA and 1.0 M NaCl) was used to dissolve all oligonucleotides and DNA hybridization buffer. 10 mM Tris-HCl (pH 7.4) including 1.0 mM EDTA, 10 mM TCEP, 0.1 M NaCl was used as HP3 immobilization buffer. Phosphate buffer saline (0.1 M PBS, pH 7.4) were prepared with $Na_2HPO_4{\cdot}12H_2O$ and $NaH_2PO_4{\cdot}2H_2O$, containing 0.1 M $K_2S_2O_8$, 0.1 M NaCl and 0.1 M KCl served as the electrolyte in ECL analysis. All solutions were prepared using Milli-Q water (18.2 MΩ·cm) from a Millipore system.

Apparatus

ECL signals were collected by a MPI-E ECL analyzer which was purchased Xi'An Remax Electronic Science & Technology Co. Ltd., China. The CV and EIS were recorded in CHI760D electrochemical workstation which was purchased from Shanghai Chenhua Apparatus Inc., China. In addition, in this work the gold electrode served as working electrode, the platinum wire served as auxiliary electrode and the Ag/AgCl saturated KCl served as a reference electrode. UV-vis absorption spectra were operated on a UV-3600 photospectrometer (Shimadzu Co., Japan). Morphology and size of nanomaterials were characterized by using JEOL 2000 transmission electron microscopy (TEM) and high resolution transmission electron microscopy (HRTEM).

Synthesis of CdSe QD

The synthesis method was similar to that described in previous work with some modification [38] are presented in the electronic supporting information(ESI).

Preparation of bio-bar-coded Au NP-CdSe quantum dots (QDs)

CdSe QDs (600 μL) were activated by 20 μL of EDC/ NHS solution (C_{EDC}/C_{NHS} = 2:1) for 20 min. The activated QDs was mixed with 80 μL of signal DNA (3 μM) with gentle shaking at 37 °C for 30 min to covalent linkage. Then the conjugates were further purified by ultrafiltration (30 kDa) to remove no bound DNA. Subsequently, the conjugates was activated with TCEP (10 μL, 10 mM) and then mixed with 40 μL of Au NPs solution with gentle shaking for 12 h. After that, the mixture was centrifugated and re-dispersed in double deionized water. The obtained product was further mixed with the TCEP (2 μL, 10 mM) activated cDNA (20 μL, 2 μM) and shaken gently for another 12 h, followed with centrifugation at 15000 rpm for 15 min. Finally, the precipitate was redispersed in dual deionized water and stored at 4 °C for next use.

Process of nicking enzyme assisted signal amplification (NESA)

Before modification, to form ideal hairpin structure, the Hairpin DNA1(HP1) and Hairpin DNA 2 (HP2) was heated to 95 °C for 5 min and then cooled slowly to room temperature, respectively. Then, the NESA was carried out by incubating the mixture of HP1(50 μL, 500 nM), a series of different concentration of UDG and HP2 (5 μL, 1 μM) in 20 μL UDG reaction buffer (200 mM Tris–HCl, 10 mM EDTA, 100 mM NaCl, pH 8.2) at 37 °C for 60 min. Then, Nb.BbvCI (2 μL, 10 $U{\cdot}\mu L^{-1}$) and 20 μL 10 × NEBuffer (50 mM KAc, 20 mM Tris acetate buffer, 10 mM magnesium acetate, 100 $\mu g{\cdot}\mu L^{-1}$ BSA, pH 7.9) were added and allowed to incubate at 37 °C for 60 min to produce a large number of intermediate sequences (S1). Finally, the above–mentioned solution was heated to 80 °C for 20 min to deactivate the Nb.BbvCI. Then the resulted products were cooled down to room temperature and stored at 4 °C for next use.

Fabrication of the electrodes

Prior to use, in order to make HP3 form stem-loop structures, the HP3 was annealed at 95 °C for 5 min and slowly cooled to room temperature. Before modification, the gold electrode (GE) (Φ = 4 mm) was polished carefully with 0.3 and 0.05 μm α-Al_2O_3 powders, respectively. The polished electrode was washed ultrasonically with water and ethanol, alternately. After this treatment, the freshly prepared piranha solution (30% H_2O_2/ 98% H_2SO_4 = 1:3, *v*/v) was dropped onto the surface of GE for 10 min. Afterward the GC was thoroughly rinsed with double deionized water. Finally, the electrode was put in a 0.5 M H_2SO_4 solution for electrochemically cleaning with

Table 1 Oligonucleotides sequence used in this work

Name	Sequence (from 5'to 3′)
Hairpin DNA1	UUCUGUAAGAAGGGA**CCTCAGC**ACAGAA
Hairpin DNA2	TTGGGTCGTTTTAATGA**GC↓TGAGG**TCCCAA
Hairpin DNA3	**AATCGT**AACAGCCGTATCTATCATTAAA**ACGATT**AAAGA-$(CH_2)_6$-SH
Hairpin DNA4	T**CAGC**TTTAATGATAGATACG**GCTG**TTACGATTGGCCTTAATT
signal DNA:	SH-$(CH_2)_6$-TTTTCAGATTCGC-$(CH_2)_6$-NH_2
cDNA:	SH-$(CH_2)_6$-TTTTAATTAAGGCC

scanning from −0.3 and 1.6 V, followed by drying under nitrogen. After that, 20 μL of 1 μM HP3 solution was modified onto surface of the GE and incubated for overnight at 4 °C to form stable Au–S bond. Next, the modified electrode was washed with deionized water and then incubated with 1 mM MCH for 30 min to eliminate nonspecific adsorption. After thoroughly washed with double deionized water, the modified electrode was stored at 4 °C for further use.

Measurement procedure

The modified electrode was then incubated with the mixture of the reaction product of NESA and HP4 (1 μM) at 37 °C for 1 h. After washing with dual distilled water, 20 μL of bio-bar-coded Au NP-CdSe QDs was modified onto the surface of electrode for further hybridization with remainder of HP4 for 2 h at 37 °C to construct the ECL signal readout. After incubation, the resultant electrodes were washed with dual deionized water to remove the physically adsorptive species. Ultimately, the obtained electrodes were analyzed by using the MPI-E ECL analyzer in PBS (0.1 M, pH 7.4) at room temperature for detection of UDG. The results showed that the ECL intensity increased with the increasing UDG concentration.

Results and discussion

Principle of the analytical process for amplified detection of UDG

In the present work, we developed an ECL biosensing platform for sensitive detection of UDG based on catalyzed hairpin assembly coupling with Nb.BbvCI assisted signal amplification, and the principle of UDG assay was shown in Scheme 1. Firstly, HP1 with four uracil (U) in the stem was used to mismatch with the the complementary strand HP1 containing adenine (A) (black color). Secondly, the detached DNA section (red color) of HP1 was complemented with the DNA section (red color) of HP 2. Here, the new assembled double strands DNA acted as the recognition sequences for the nicking enzymes Nb.BbvCI. Thirdly, in HP2, the green DNA sequence was designed as a complementary domain of HP3, which could combine with HP4 participating in CHA recycling process. In summary, this biosensor assay includes three steps:(1) UDG induced uracil-excision repair reaction and Nb.BbvCI nicking enzymes assisted signal amplification, (2) intermediate sequences (S1) catalyzed hairpin assembly reaction, and (3) bio-bar-coded Au NP-CdSe QDs as signal ECL probes provided ECL signal. Here, UDG can specially recognizes the uracil bases and hydrolyzes it from the stem of HP1 which can cleave the N-glycosidic bond between the sugar and uracil, resulting in remove of the uracil and formation of abasic site (AP site). Because of the instability of the stem with AP sites, HP 1 was easily opened and can further hybridize with DNA region (red color) of HP 2. The resulted double-stranded structure exhibited a recognition site for the Nb.BbvCI. Additionally, the Nb.BbvCI cleaved the specific DNA sequences on cleavage site (5'-GC↓TGAGG-3′), bringing about the release of the HP 1 and the generation of intermediate sequences (S1) (Scheme 1). In the meantime, the detached HP1 hybridized with other HP2 to trigger frequent cycle of cleavage, eventually resulting in production of plentiful S1. Secondly, the introduction of S1 could hybridize with HP3 modified on the GE surface to form dsDNA and further induce the exposure of the complementary sequence of HP3, which can hybridize with HP4. When the HP4 existed in this hybridization system, the HP3 combines with HP4 by a branch migration process. Because HP3–HP4 possessed longer and more stable complementary sequence than HP3–S1 hybrid chains, the HP4 would supersede and release the S1 when it hybridizes with HP3. The freed S1 would trigger the next cycle to capture a mass of HP3. Thirdly, the redundant part of opened HP4 can hybridize with the cDNA modified on the bio-bar-coded Au NP-CdSe QDs serving as ECL signal probe which can generate a strong ECL signal. In brief, the sensitivity of the biosensor was obviously enhanced after introducing Nb.BbvCI nicking enzymes, CHA intermediate sequences recycling, and bio-bar-coded Au NP-CdSe QDs.

Characterization of the different nanomaterials

Figure 1a shows the TEM image of CdSe QDs, it is obvious to observe that particle size distributes homogeneous with an average diameter of 4.5 nm. The HRTEM of CdSe QDs is shown in Fig. 1b, which behaves highly crystalline and uniform lattice fringes distribution. Figure 1c shows the HRTEM image of Au nanoparticles (Au NPs), as is described in the image, the average diameter of Au NPs is about 15 nm, which is beneficial for the connection of signal DNA and cDNA by Au-S bond. UV-vis spectroscopy were used in this work to certify successful combination of CdSe QDs with Au NPs. As shown in Fig. 1d, two absorption peaks at 263 nm and 435 nm are assigned to special peaks of DNA and CdSe QDs, respectively. Compared with UV-vis spectrum of CdSe QDs-DNA, the biobar-coded Au NPs-CdSe QDs exhibits a new peak at 523 nm, which attributs to the characteristic absorption of Au NPs and indicates the successful attachment of CdSe QDs onto the surface of Au NPs.

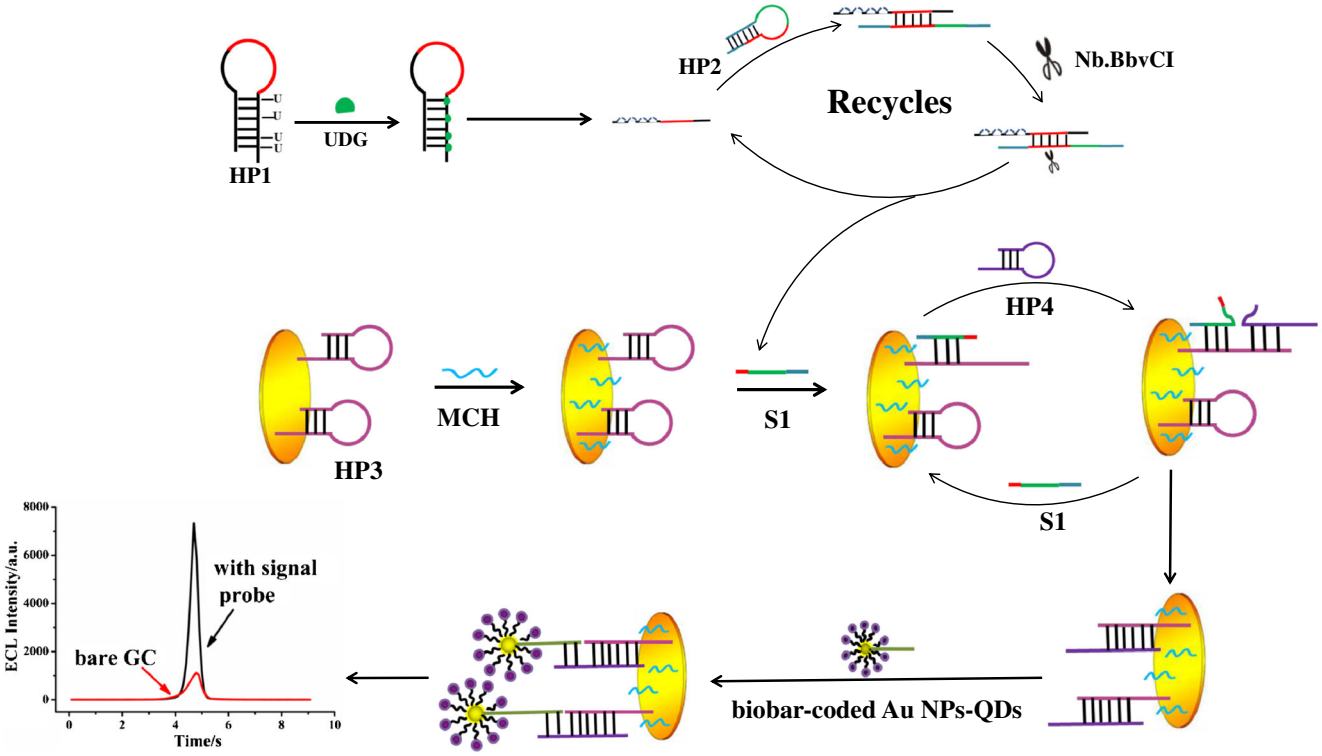

Scheme 1 Schematic illustration of the principle of the ECL biosensor for detection of the activity of UDG

EIS and CV characterization of stepwise fabrication of the proposed biosensor

EIS as an important tool was utilized to study the interface properties of different electrodes. It can be seen from Fig. 2a, the bare GE behaved a smaller semicircle (curve a), implying the good electrical conductivity of the electrode. When HP3 (curve b) and MCH (curve c) were modified on the GE, successively, the semicircle turned into larger than the bare GE because of the electrostatic repulsive force between the negatively charged DNA backbones and the $Fe(CN)_6]^{3-/4-}$ redox probe, which impeded the electron transport. Additionally, this semicircle further increased after the modified electrode was incubated in the mixture of S1 and HP4, which was assigned to the successful catalyzed hairpin assembly process (curve d). And the fact also indicated that more DNA strands with negatively charged were immobilized on the electarode surface, hindering the diffusion of $Fe(CN)_6]^{3-/4-}$. Then the semicircle increased obviously after immobilizing bio-bar-coded Au NPs-CdSe QDs (curve e), on account of the enlargement of steric hindrance.

CV was also used to investigate the assembly process of the modified electrodes. It can be seen from Fig. 2b, the bare GC displayed a pair of explicit redox peaks (curve a). After successive assembling of the HP3 and MCH on the surface of GE, the redox peak currents decreased obviously (curve b and curve c). The reason was that the MCH and DNA stands insulate the redox probe resulting in the difficult electron transfer. After incubating the mixture of S1 and HP4 (curve d), the oxidation and reduction peak currents further decreased because $Fe(CN)_6]^{3-/4-}$ encountered difficult diffusion toward the electrode surface. Afterwards, when the prepared electrode was incubated with bio-bar-coded Au NPs- CdSe QDs (curve e), the oxidation and reduction peak currents was decreased remarkably. The CV results were consistent with EIS, which manifested that the ECL biosensor was constructed successfully.

Optimization of experimental conditions

The following parameters were optimized: (a) Concentration of HP1; (b) Nb.BbvCI cleavage time; (c) concentration of Nb.BbvCI; (d) recycling time. Respective data and Figures (Fig. S2) are given in the Supporting information. The following experimental conditions were found to give best results: (a) Best concentration of HP1: 500 nM; (b) Optimal Nb.BbvCI cleavage time: 60 min; (c) Best concentration of Nb.BbvCI: 20 U; (d) Recycling time was 60 min.

Analytical performance of the assay

Based on optimized conditions, the quantitative detection of UDG activity was carried out in this work. As the concentration of UDG increased, more S1 sequences broke

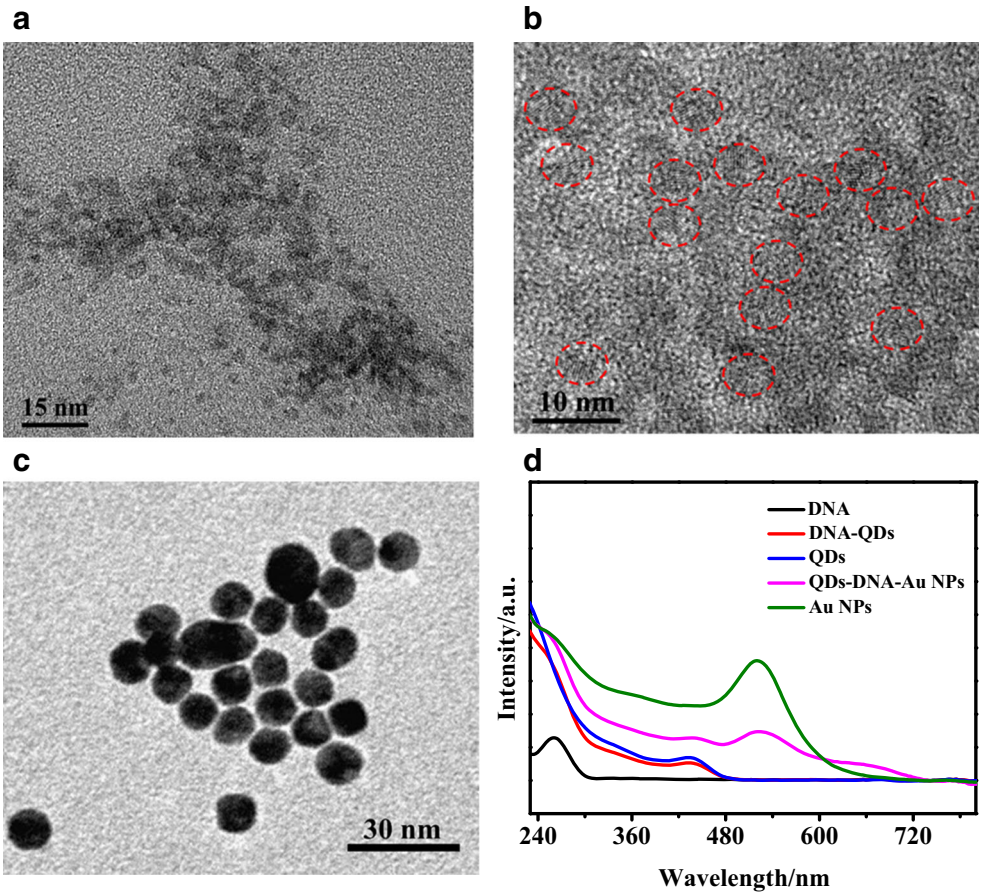

Fig. 1 **a** TEM image of the CdSe QDs; **b** HRTEM image of the CdSe QDs; **c** TEM images of Au NPs; **d** UV − vis extinction spectra of DNA, CdSe QDs, DNA-CdSe QDs, Au NPs, and Au-DNA-CdSe QDs

away from the heteroduplex and more HP3 was opened in the presence of HP4, causing more bio-bar-coded Au NP-CdSe QDs immobilizing onto the electrode surface. The ECL signal gradually increased with increasing concentrations of UDG (curves a-i) (Fig. 3a). As shown in Fig. 3b, the quantitative determination of UDG was displayed in calibration plots. The ECL intensity was proportional to the logarithm concentration of UDG and the

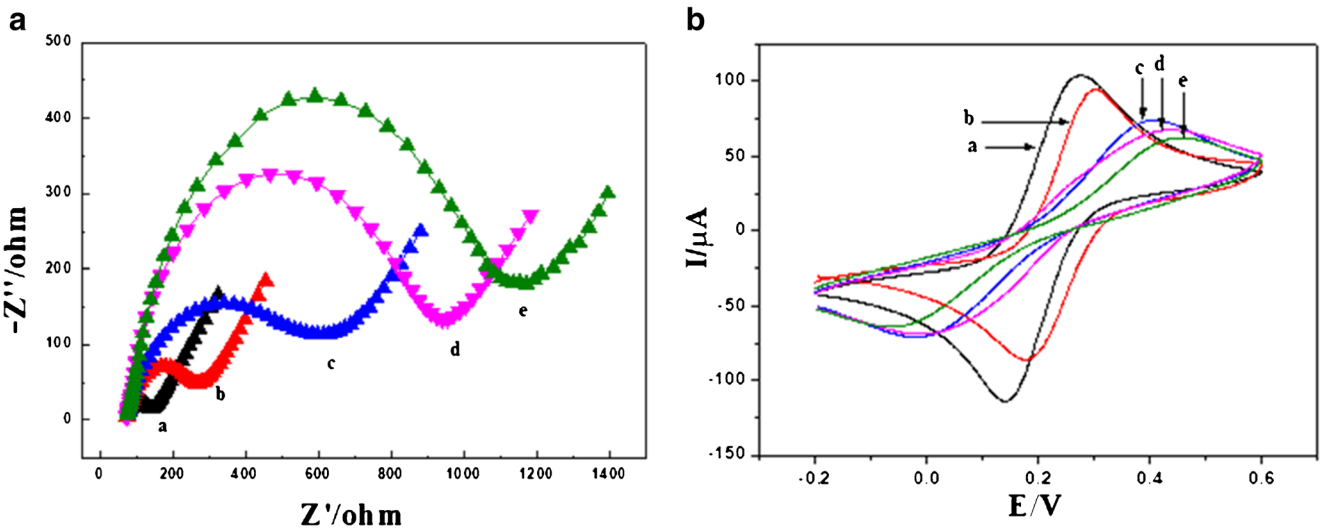

Fig. 2 EIS (**a**) and CV (**b**) of modified Au electrode at different stages: (a) bare GE, (b) HP3/GE, (c) MCH/HP3/GE, (d) HP4/MCH/HP3/GE and (e) biobar-coded Au NPs-CdSeQDs /HP2/MCH/HP3/GE in 5 mM $Fe(CN)_6^{3-/4-}$ containing 0.1 M KCl. The frequency range for EIS: 0.1–1.0 × 10^5 Hz. The scan range and scan rate for CV is −0.2 to 0.6 V and 100 mV/s, respectively

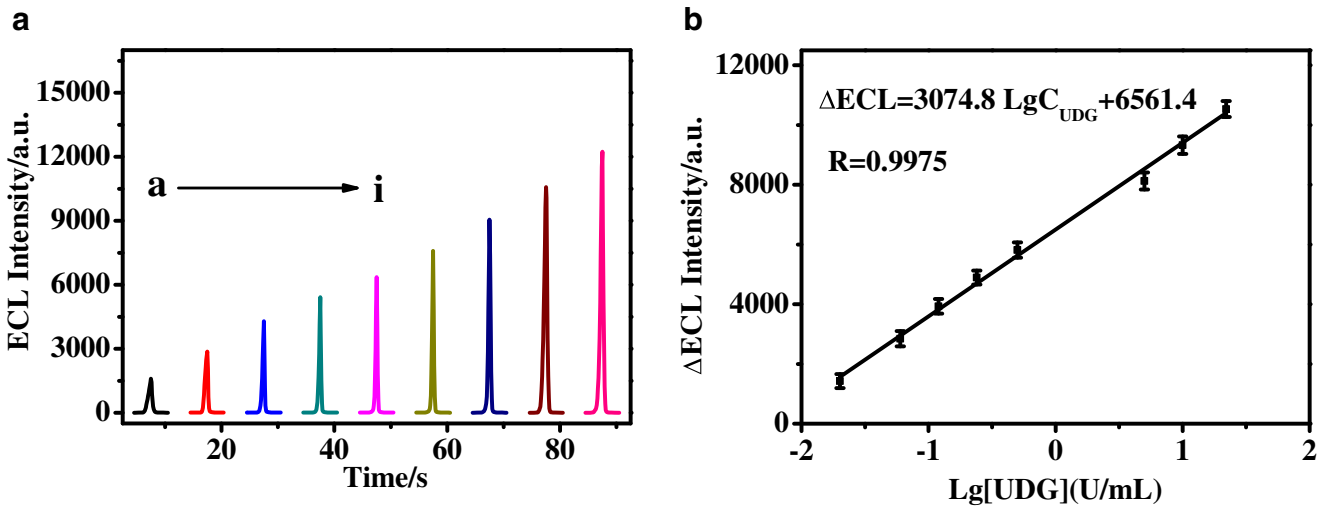

Fig. 3 **a** ECL intensity-Time curves of the proposed biosensors under different concentrations of UDG: (a) 0, (b) 0.02, (c) 0.06, (d) 0.12, (e) 0.24, (f) 0.5, (g) 5, (h) 10 and (i) 22 U·mL^{-1}. **b** ECL intensities of biosensor in the presence of UDG at varying concentrations. Inset: the calibration plot of ΔECL (ΔECL = ECL - ECL$_0$) vs the logarithm of UDG concentration. Error bars represent standard deviations of three independent experiments. The potential scanning was set from −1.5 to 0 V with a scan rate of 0.3 V/s

linear range for UDG was 0.02 U·mL^{-1}–22 U·mL^{-1}. Moreover, the detection limit was 0.006 U·mL^{-1}(S/*N* = 3) which was lower than that of the previously reported UDG activity assay (Table 2). The linear equation was described as ΔECL = 3074.8 Lg C_{UDG} + 6561.4 with the correlation coefficient of 0.9975, where ΔECL (ΔECL = ECL - ECL$_0$) represented the change of ECL intensity and C was the UDG concentration. This biosensor possess superior sensitivity, which can be explained as follows: (1) the specific uracil-excision repair induced by UDG, (2) the excellent amplification efficiency assisted by Nb.BbvCI nicking enzymes and employment of CHA intermediate sequences recycling, and (3) bio-bar-coded Au NP-QDs as signal readout achieving further signal amplification.

Specificity, stability, and reproducibility of the assay

To evaluate the specificity of the developed biosensor, we employed hOGG1, hAAG and nonspecific Cyt C as interferences study. The same concentration of hOGG1, hAAG and Cyt C was used to replace UDG. It was shown that the relative ECL signal was very low in comparison with the blank test in the presence of hOGG1, hAAG and Cyt C (Fig. 4a). Moreover, when ten times of the above interferences were mixed with the 4 U·mL^{-1} UDG solution, the ECL intensity was as high as that in the system containing UDG only. The above results indicated that the proposed biosensor had unexceptionable specificity for detection of UDG. The admirable specificity of this assay was mainly on account of the specific site recognition of UDG toward its substrate.

In addition, the stability of the biosensor were further researched. Through using one proposed biosensor for 22 consecutive cyclic scans in PBS (pH 7.4), as seen from Fig. 4b, the ECL response behaved wonderful uniformity and the relative standard deviation (RSD) was 2.69%, manifesting accredited stability toward UDG detection. Furthermore, the long-time reserve stability of this biosensor was also researched in a period of 25 days. The as-modified electrode of thirty were reserved at 4 °C. Afterward, five biosensors were taken out to measure the ECL signal in PBS (pH 7.4) for every 5 days. The results indicated the biosensor retained 94.99% of its initial ECL signal after 15 days reserve and 80.09% after 25 days reserve (Fig. 4c). Therefore, the above phenomenon exhibited that prepared biosensor had good stability. In addition, in order to evaluate the reproducibility of the biosensor,

Table 2 Comparison of the current approach and previous reports on the detection of UDG

Measurement Method	Linear Range (U/mL)	Detection limit (U/mL)	Reference
colorimetric	0.06–8	0.02	[29]
fluorometric	0–1	0.02	[41]
colorimetric	0.008–0.2	0.008	39
fluorometric	0.01–1	0.0078	40
Electrochemiluminescent	0.02–22	0.006	This work

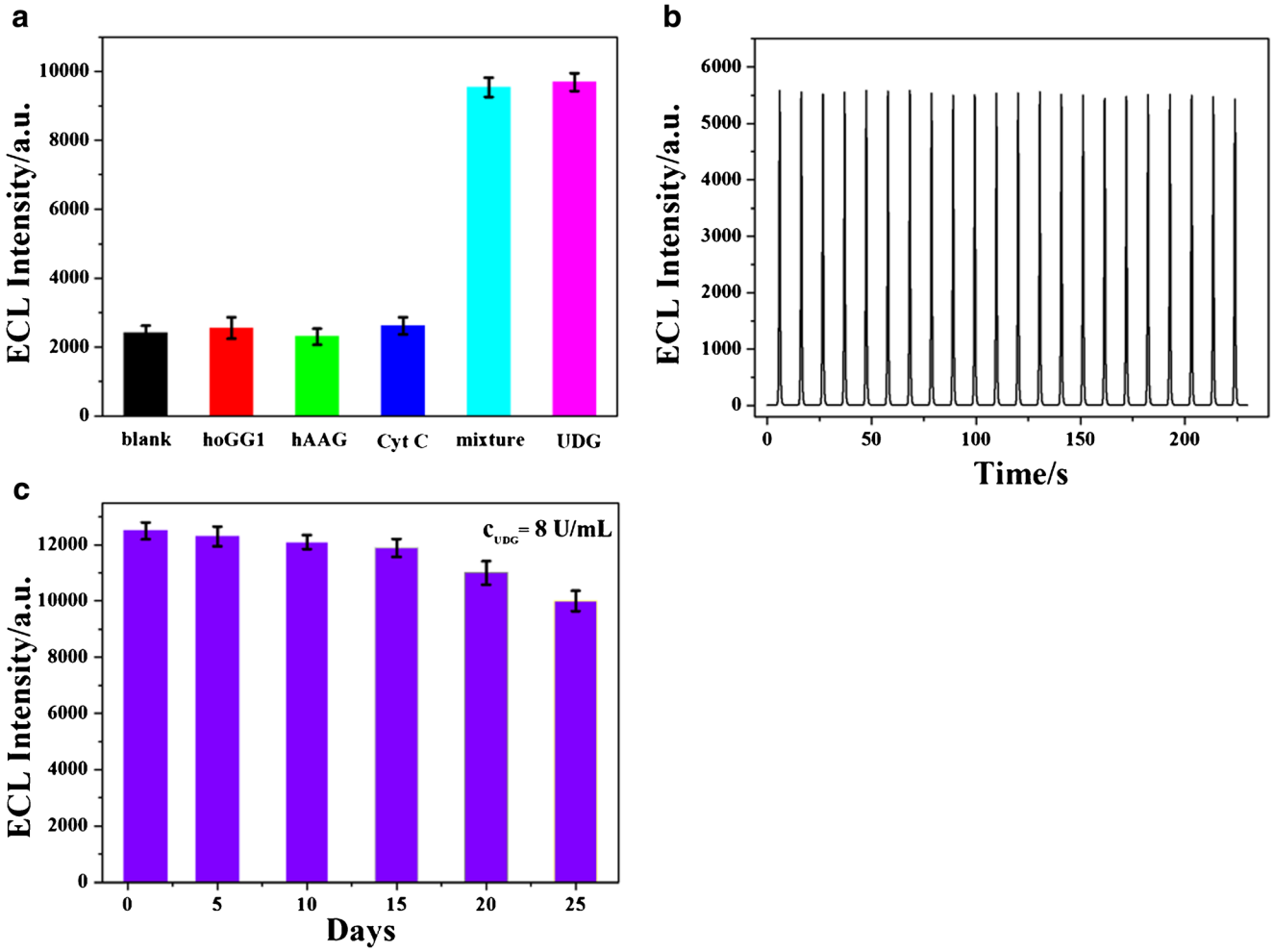

Fig. 4 **a** Specificity of the assay: hOGG1 (20 U·mL^{-1}), hAAG (20 U·mL^{-1}), Cyt C (20 U·mL^{-1}), UDG (5 U·mL^{-1}) and a mixture containing 20 U·mL^{-1} hOGG1, 20 U·mL^{-1} hAAG, 20 U·mL^{-1} Cyt C, 5 U·mL^{-1} UDG. **b** Stability of the proposed biosensor under consecutive 22 cyclic potential scans. **c** The storage stability of the proposed biosensor. Error bars represent standard deviations of three independent experiments. The potential scanning was set from −1.5 to 0 V with a scan rate of 0.3 V/s

five modified electrodes were investigated in the same conditions. The relative standard deviation (RSD) of measurements was 4.8% for the detection UDG, demonstrating the well reproducibility.

Conclusions

We describe a novel and highly sensitive ECL biosensor for amplified detection of UDG by Nb.BbvCI assisted signal amplification coupled with catalyzed hairpin assembly. This strategy had several excellent advantages. First, this method for the first time utilized amplification strategies based on both nicking enzyme assisted recycling and catalyzed hairpin assembly into one ECL system for the UDG detection. Second, bio-bar-coded Au NPs for QDs enrichment as ECL signal recorder further achieved signal amplification. Third, this sensing system has high selectivity and sensitivity, and thus behaves unexceptionable performance compared to those previously reported colorimetric-based [39] or fluorescence-based assays [40]. Furthermore, the strategy was also applied to detect trace UDG in fetal bovine serum, proving better practical application value. These results indicated that the developed strategy was feasible and will be used in UDG-related function study and disease prognosis. Although, this stragety needed traditional electrodes, which limted this universality. But we believe that the portable equipments and UDG-chip sensors will meet the in-situ and low sample consumed detection according to the similar way we proposed.

Acknowledgements We are grateful to Natural Science Research Key Project of Education Department of Anhui Province (No. KJ2018A0453,

KJ2017A434, KJ2017A435 and KJ2018A0446) and Academic Technical Leader of Suzhou University (No. 2016xjxs03 and 2016msgzs071) for funding this work. The authors also thank the Key Discipline of Material Science and Engineering of Suzhou University (No. 2017XJZDXK3) and Innovative Research Team of Anhui Provincial Education Department (No. 2016SCXPTTD) for supporting this work.

Compliance with ethical standards The author(s) declare that they have no competing interests.

References

1. van Loon AAWM, Sonneveld E, Hoogerbrugge J, van der Schans GP, Grootegoed JA, Lohman PHM, Baan RA (1993) Induction and repair of D N A single-strand breaks and D N A base damage at different cellular stages of spermatogenesis of the hamster upon in vitro exposure to ionizing radiation. Mutat Res, DNA Repair 294:139–148
2. Giovannelli L, Pitozzi V, Moretti S, Boddi V, Dolara P (2006) Seasonal variations of DNA damage in human lymphocytes: correlation with different environmental variables. Mutat Res 593: 143–152
3. Papachristou F, Simopoulou M, Touloupidis S, Tsalikidis C, Sofikitis N, Lialiaris T (2008) DNA damage and chromosomal aberrations in various types of male factor infertility. Fertil Steril 90:1774–1781
4. Krokan HE, Drabløs F, Slupphaug G (2002) Uracil in DNA – occurrence, consequences and repair. Oncogene 21:8935–8948
5. Krokan HE, Standal R, Slupphaug G (1997) DNA glycosylases in the base excision repair of DNA. Biochem J 325:1–16
6. Impellizzeri KJ, Anderson B, Burgers PMJ (1991) The Spectrum of spontaneous mutations in a Saccharomyces cerevisiae uracil-DNA-glycosylase mutant limits the function of this enzyme to cytosine deamination repair. J Bacteriol 173:6807–6810
7. Lindahl T (1974) An N-Glycosidase from Escherichia coli that releases free uracil from DNA containing Deaminated cytosine residues. Proc Natl Acad Sci U S A 71:3649–3653
8. Wallace SS (2014) Base excision repair: a critical player in many games. DNA Repair 19:14–26
9. Duncan BK, Miller JH (1980) Mutagetic deamination of cytosine residues in DNA. Nature 287:560–561
10. Wang Y, Wang Y, Li D, Xu J, Ye C (2018) Detection of nucleic acids and elimination of carryover contamination by using loop-mediated isothermal amplification and antarctic thermal sensitive uracil-DNA-glycosylase in a lateral flow biosensor: application to the detection of Streptococcus pneumonia. Microchim Acta 185:212
11. Wu YS, Yan P, Xu XW, Jiang W (2016) A unique dual recognition hairpin probe mediated fluorescent amplification method for sensitive detection of uracil-DNA glycosylase and endonuclease IV activities. Analyst 141:1789–1795
12. Sousa MML, Krokan HE, Slupphaug G (2007) DNA-uracil and human pathology. Mol Asp Med 28:276–306
13. Sung JS, Mosbaugh DW (2000) Escherichia coli double-Strand uracil-DNA glycosylase: involvement in uracil-mediated DNA Base excision repair and stimulation of activity by endonuclease IV. Biochemistry 39:10224–10235
14. Duthie SJ, McMillan P (1997) Uracil misincorporation in human DNA detected using single cell gel electrophoresis. Carcinogenesis 18:1709–1714
15. Krokan H, Wittwer CU (1981) Uracil DNA-glycosylase from HeLa cells: general properties, substrate specificity and effect of uracil analogs. Nucleic Acids Res 9:2599–2613
16. Wang LJ, Ren M, Zhang QY, Tang B, Zhang CY (2017) Excision repair-initiated enzyme-assisted bicyclic Cascade signal amplification for ultrasensitive detection of uracil-DNA glycosylase. Anal Chem 89:4488–4494
17. Richter MM (2004) Electrochemiluminescence (ECL). Chem Rev 104:3003–3036
18. Shi CG, Shan X, Pan ZQ, Xu JJ, Lu C, Bao N, Gu HY (2012) Quantum Dot (QD)-modified carbon tape electrodes for reproducible Electrochemiluminescence (ECL) emission on a PaperBased platform. Anal Chem 84:3033–3038
19. Liu Q, Ma C, Liu XP, Wei YP, Mao CJ, Zhu JJ (2017) A novel electrochemiluminescence biosensor for the detection of microRNAs based on a DNA functionalized nitrogen doped carbon quantum dots as signal enhancers. Biosens Bioelectron 92:273–279
20. Wang MH, Zhou YL, YL YHS, Jiang WJ, Wang HY, Ai SY (2018) Signal-on electrochemiluminescence biosensor for microRNA-319a detection based on two-stage isothermal strand-displacement polymerase reaction. Biosens Bioelectron 107:34–39
21. Liu Q, Yang Y, Liu XP, Wei YP, Mao CJ, Chen JS, Niu HL, Song JM, Zhang SY, Jin BK, Jiang M (2017) A facile in situ synthesis of MIL-101-CdSe nanocomposites for ultrasensitive electrochemiluminescence detection of carcinoembryonic antigen. Sensors Actuators B Chem 242:1073–1078
22. Hu XW, Mao CJ, Song JM, Niu HL, Zhang SY, Huang HP (2013) Fabrication of GO/PANi/CdSe nanocomposites for sensitive electrochemiluminescence biosensor. Biosens Bioelectron 41: 372–378
23. Cheng CM, Huang Y, Tian XQ, Zheng BZ, Li Y, Yuan HY, Xiao D, Xie SP, Choi MMF (2012) Electrogenerated Chemiluminescence behavior of graphite-like carbon nitride and its application in selective sensing Cu^{2+}. Anal Chem 84:4754–4759
24. Zhou ZX, Shang QW, Shen YF, Zhang LQ, Zhang YY, Lv YQ, Li Y, Liu SQ, Zhang YJ (2016) Chemically modulated carbon nitride Nanosheets for highly selective Electrochemiluminescent detection of multiple metal-ions. Anal Chem 88:6004–6010
25. Chan SH, Stoddard BL, Xu SY (2011) Natural and engineered nicking endonucleases-from cleavage mechanism to engineering of strand-specificity. Nucleic Acids Res 39:11–18
26. Kuhn H, Kamenetskii MDF (2008) Labeling of unique sequences in double-stranded DNA at sites of vicinal nicks generated by nicking endonucleases. Nucleic Acids Res 36:e40
27. Bi S, Zhang JL, Zhang SS (2010) Ultrasensitive and selective DNA detection based on nicking endonuclease assisted signal amplification and its application in cancer cell detection. Chem Commun 46: 5509–5511
28. Zhu XL, Zhao J, Wu Y, Shen ZM, Li GX (2011) Fabrication of a highly sensitive Aptasensor for potassium with a nicking endonuclease-assisted signal amplification strategy. Anal Chem 83:4085–4089
29. Liu XJ, Chen MQ, Hou T, Wang XZ, Liu SF, Li F (2014) Label-free colorimetric assay for base excision repair enzyme activity based on nicking enzyme assisted signal amplification. Biosens Bioelectron 54:598–602
30. Zhang PP, Wang L, Zhao HY, Xua XW, Jia W (2017) Self-primer and self-template recycle rolling circle amplification strategy for sensitive detection of uracil-DNA glycosylase activity. Anal Chim Acta 1001:119–124
31. Kong XJ, Wu S, Cen Y, Yu RQ, Chu X (2016) "Light-up" sensing of human 8-oxoguanine DNA glycosylase activity by target-

induced autocatalytic DNAzyme-generated rolling circle amplification. Biosens Bioelectron 79:679–684
32. Wu YS, Wang L, Jiang W (2016) Toehold-mediated strand displacement reaction-dependent fluorescent strategy for sensitive detection of uracil-DNA glycosylase activity. Biosens Bioelectron 89: 984–988
33. Zheng AX, Li J, Wang JR, Song XR, Chen GN, Yan HH (2012) Enzyme-free signal amplification in the DNAzyme sensor via target-catalyzed hairpin assembly. Chem Commun 48: 3112–3114
34. Li YL, Yu C, Yang B, Liu ZR, Xia PY, Wang Q (2018) Target-catalyzed hairpin assembly and metal-organic frameworks mediated nonenzymatic co-reaction for multiple signal amplification detection of miR-122 in human serum. Biosens Bioelectron 102:307–315
35. Wu XY, Chai YQ, YQ ZP, Yuan R (2015) An electrochemical biosensor for sensitive detection of MicroRNA-155: combining target recycling with Cascade catalysis for signal amplification. ACS Appl Mater Interfaces 7:713–720
36. Liu SF, Wang Y, Ming JJ, Lin Y, Cheng CB, Li F (2013) Enzyme-free and ultrasensitive electrochemical detection of nucleic acids by target catalyzed hairpin assembly followed with hybridization chain reaction. Biosens Bioelectron 49:472–477
37. Lin DJ, Wu J, Yan F, Deng SY, Ju HX (2011) Ultrasensitive immunoassay of protein biomarker based on Electrochemiluminescent quenching of quantum dots by hemin bio-Bar-coded nanoparticle tags. Anal Chem 83:5214–5221
38. Liu XL, Ma CC, Yan Y, Yao GX, Tang YF, Huo PW, Shi WD, Yan YS (2013) Hydrothermal synthesis of CdSe quantum dots and their photocatalytic activity on degradation of Cefalexin. Ind Eng Chem Res 52:15015–15023
39. Nie HJ, Wang W, Li W, Nie Z, Yao SZ (2015) A colorimetric and smartphone readable method for uracil-DNA glycosylase detection based on the target-triggered formation of G-quadruplex. Analyst 140:2771–2777
40. Zhang XF, Li N, Ling Y, Tang L, Li NB, Luo HQ (2018) Linked bridge hybridizing-induced split G quadruplex DNA machine and its application to uracil-DNA glycosylase detection. Sensors Actuators B Chem 255:2589–2594
41. Lee CY, Parka KS, Park HG (2015) Fluorescent G-quadruplex probe for the assay of base excision repair enzyme activity. Chem Commun 51:13744–13747